Supplementary Information

Condensin Accelerates Long-Range Intra-Chromosomal Interactions

Fan Zou[1,2*], Yi Li[2,3*], Timothy Földes[4*], Henrik Dahl Pinholt[4], Courtney Smith[2,3], Leonid Mirny[4], Lu Bai[1,2,3†]

[1]Department of Physics, [2]Center for Eukaryotic Gene Regulation, [3]Department of Biochemistry and Molecular Biology, The Pennsylvania State University, University Park, PA 16802, USA, [4]Institute for Medical Engineering and Science, Massachusetts Institute of Technology, Cambridge, MA, USA

* These authors contributed equally to this work

† Corresponding author, Email: lub15@psu.edu

Supplementary Information includes:

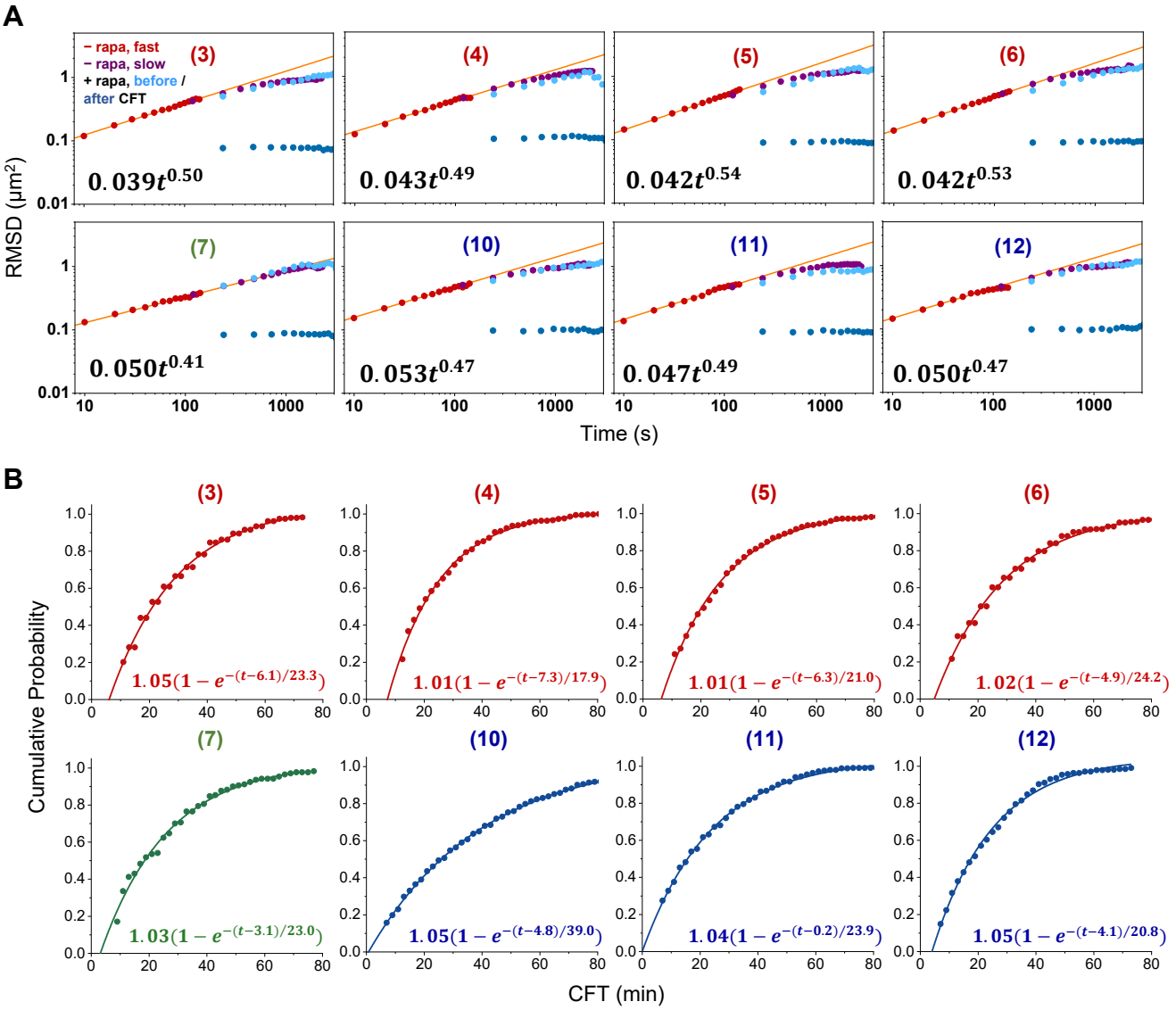

Supplementary Fig. 1. RMSDs and CFTs of more loci pairs. A) RMSDs as a function of time for intra-arm pairs 3-6, inter-arm pair 7, and inter-chromosomal pairs 10-12. Best power-law fits for the shorter time points are shown in the diagram. **B)** Cumulative CFT probabilities for the same pairs in A. The single exponential fit is shown in each panel.

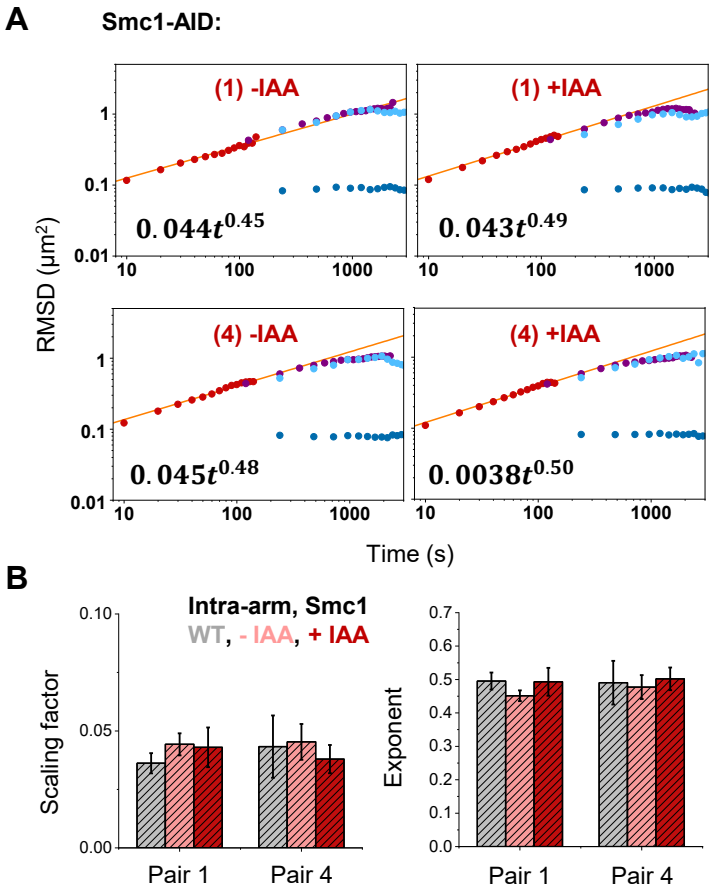

Supplementary Fig. 2. Smc1 depletion has little effect on chromosome motion. A) RMSDs as a function of time in Smc1-AID strain ±IAA for pair 1 and 4. **B)** The best-fit scaling factor and exponent of the RMSDs in WT and Smc1-AID strain ±IAA for pair 1 and 4.

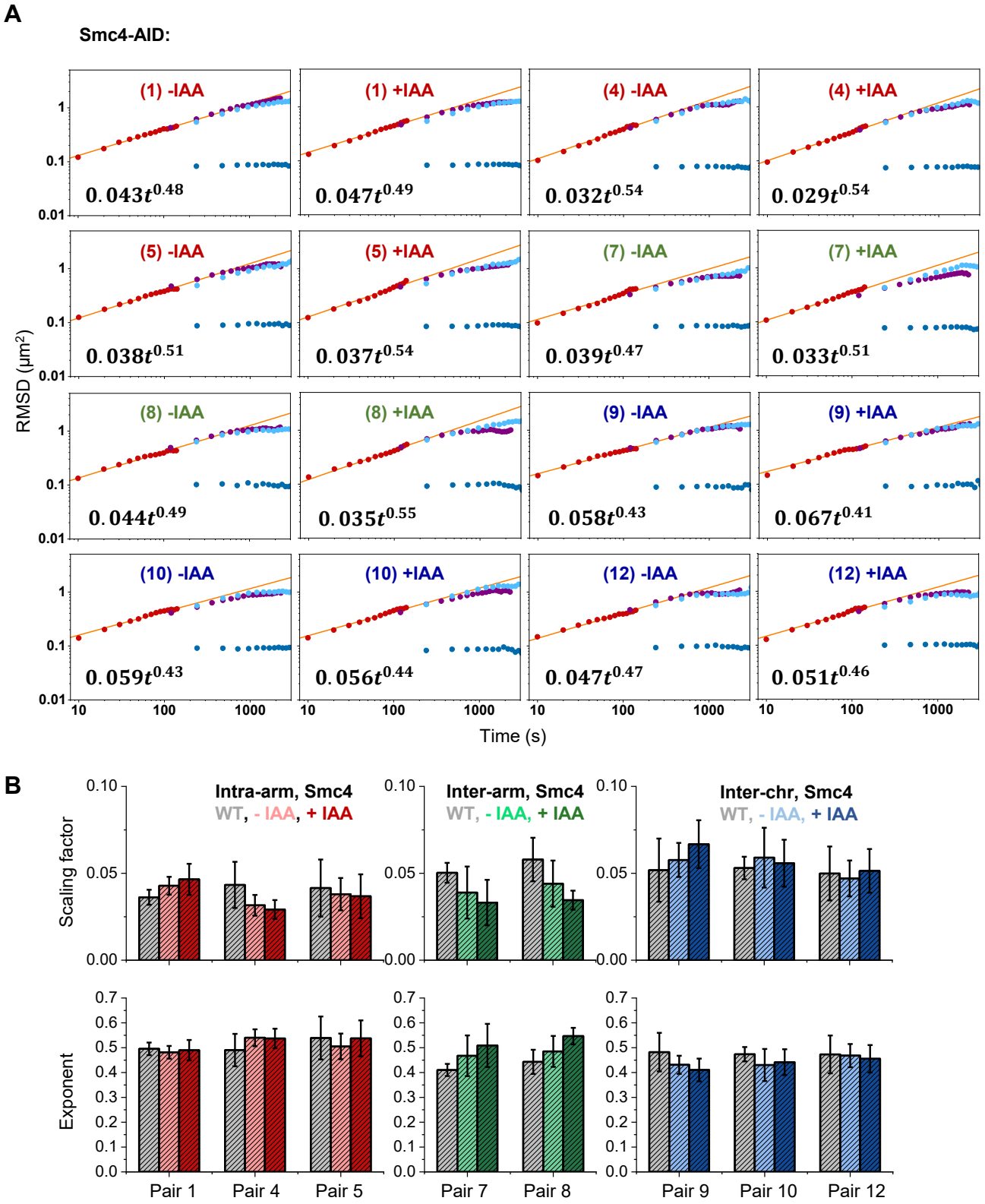

Supplementary Fig. 3. Smc4 depletion has little effect on chromosome motion. A) RMSDs as a function of time in Smc4-AID strain ±IAA for indicated pairs. **B)** The best-fit scaling factor (top) and exponent (bottom) of the RMSDs in WT and Smc4-AID strain ±IAA for indicated pairs.

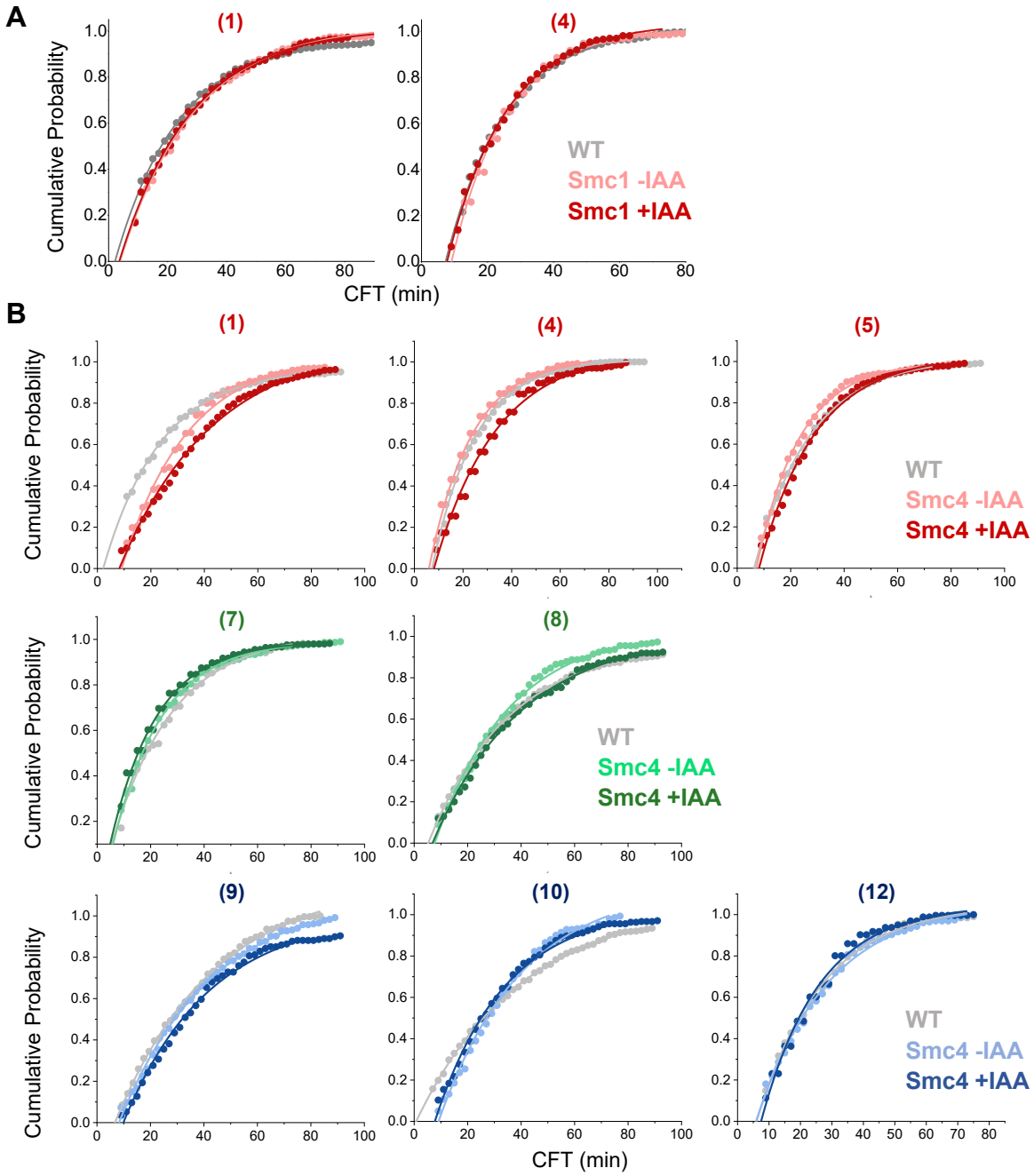

Supplementary Fig. 4. CFTs in Smc1/Smc4 depletion strains. A) Cumulative CFT probabilities in WT and Smc1-AID strain ±IAA for pair 1 and 4. **B)** Cumulative CFT probabilities in WT and Smc4-AID strain ±IAA for indicated pairs.

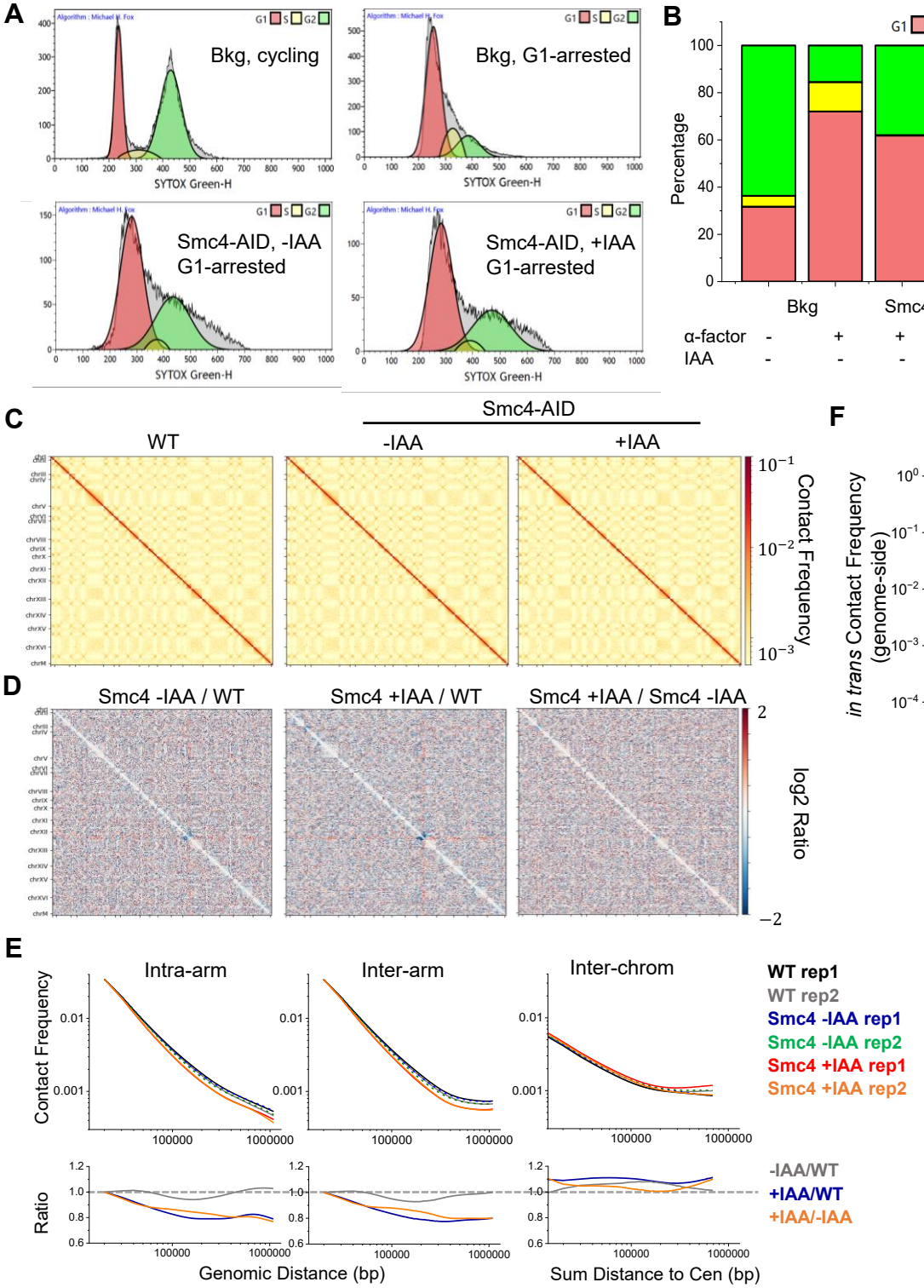

Supplementary Fig. 5. Condensin effect on genome-wide chromosome conformation in G1 yeast. A) FACS profiles showing DNA content in the parental CICI strain (containing pair 4) under cycling and G1-arrested conditions, as well as in the derived Smc4-AID strain with or without Smc4 degradation. **B)** Quantification of G1, S, and G2 populations based on the fitting of FACS profiles in panel A. **C)** Genome-wide Hi-C contact matrices in G1-arrested WT and Smc4-AID strain ±IAA. **D)** log2 fold change of the data in A. **E)** Contact frequency vs linear genomic distance in WT (black) and condensin-depleted (red) G1 cells. Upper panels show the contact frequencies averaged across the genome as a function of genomic distances, and the lower panels show the Smc4 ±IAA / WT and Smc4+IAA/-IAA ratio. The left two columns represent loci pairs on the same chromosome arms or on the same chromosome but on different arms. The right column represents inter-chromosomal loci pairs with the same distance (x axis) to their corresponding centromeres. **F)** Contact frequencies between all possible inter-chromosomal loci pairs in WT and Smc4-AID strain ±IAA.

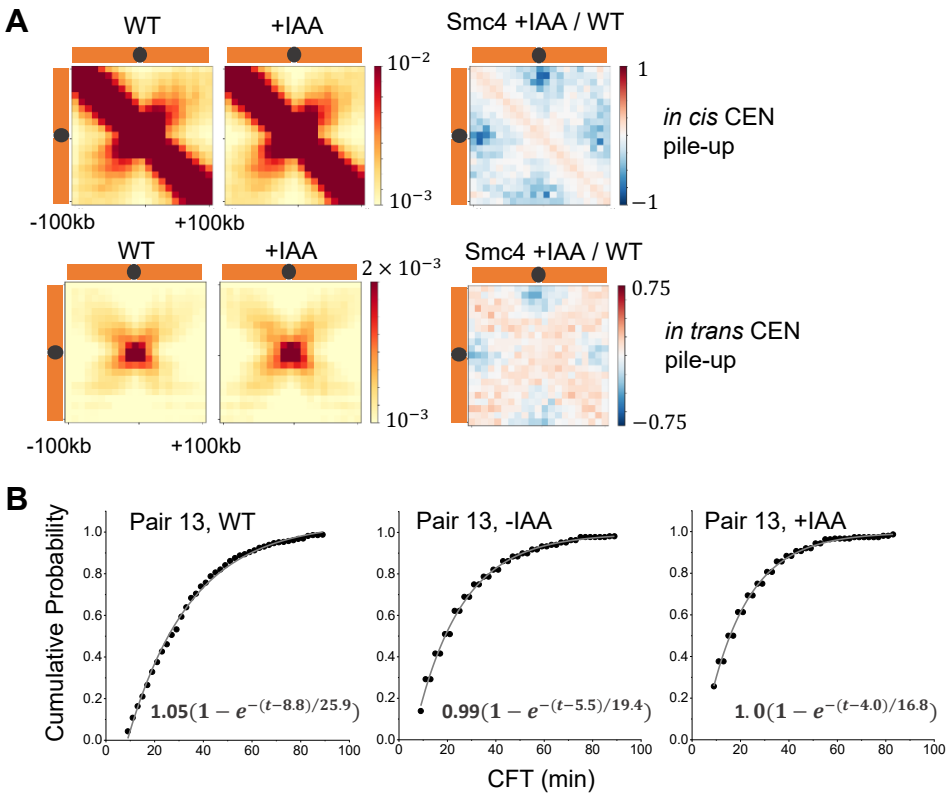

Supplementary Fig. 6. Condensin effect on Hi-C and CFT in specialized genomic region. **A)** Pile-ups of the Hi-C contact matrices of ±100kb regions centered around centromeres in in WT vs Smc4-depleted cells. log2 fold change between Smc4-AID +IAA and WT is shown on the right. **B)** Cumulative CFT probabilities in WT strain and Smc4-AID strain ±IAA for pair 13.

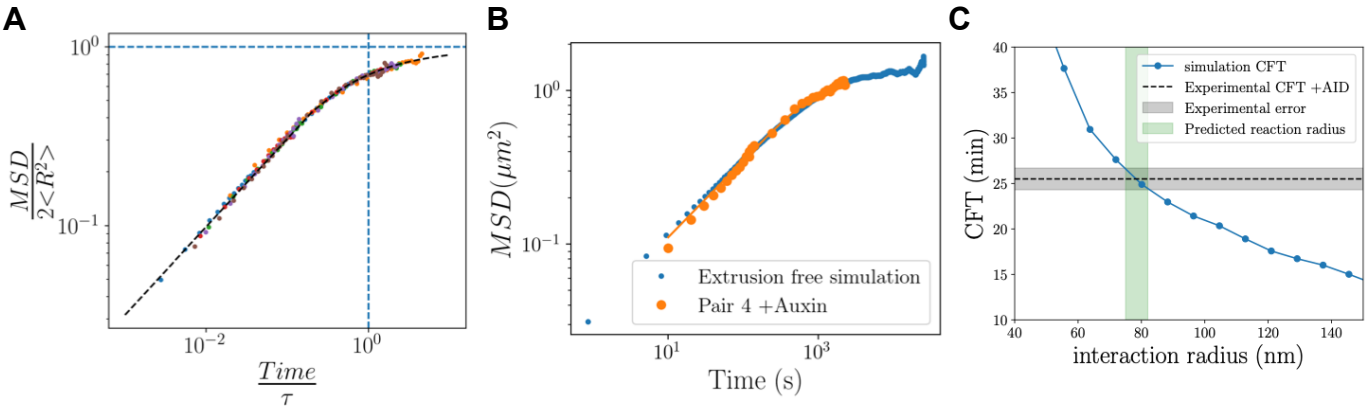

Supplementary Fig. 7. Rescaling procedure for mapping simulation length scales to experimental data.
A) Experimental two-point MSD data for multiple WT and condensin depleted pairs, collapsed onto a single curve by rescaling time with the fitted Rouse time and MSD with the squared fitted spatial separation, R^2. The rescaling parameters, Rouse time and R, were obtained by fitting the theoretical two-point MSD for a Rouse chain (Equation: $M_2(t)$ **B)** Experimental RMSD for locus pair 4 in condensin-depleted cells, overlaid with the corresponding rescaled simulation data. This comparison ensures that the simulation units are properly scaled to match the experimental RMSD. **C)** Search time computed in simulations without extrusion for different values of the array interaction radius. The gray dashed line represents the experimental search time for locus pair 4 in condensin-depleted cells, with the shaded region indicating the corresponding error bar. The vertical green shaded region marks the fitted interaction radius, determined as the value that best matches the experimental search time.

$$M_2(t) = 2\Gamma_2\sqrt{t}\left(1 - \exp\left(-\frac{\tau}{\pi t}\right)\right) + 2J\mathrm{erfc}\left(\sqrt{\frac{\tau}{\pi t}}\right)$$

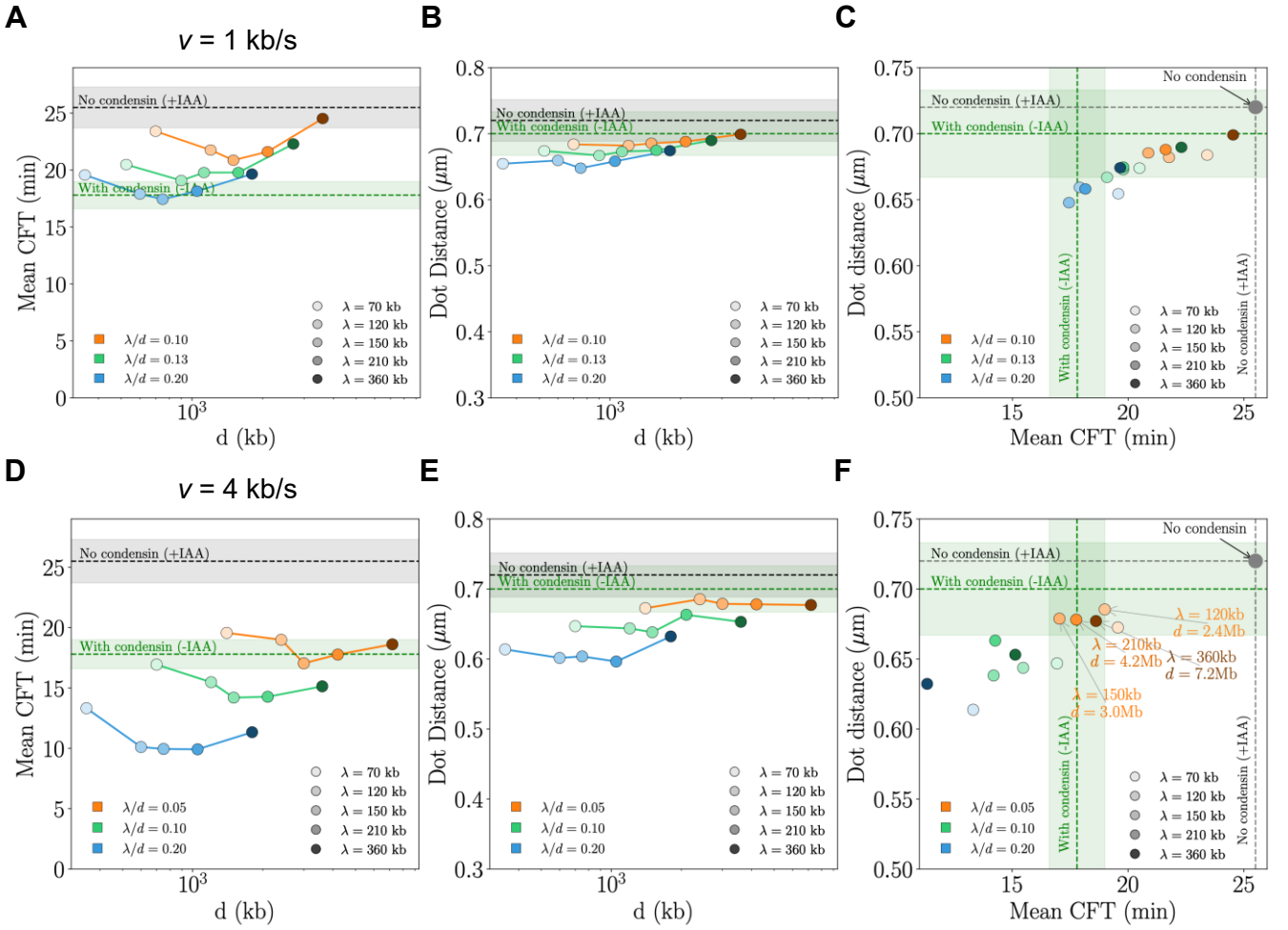

Supplementary Fig. 8. Simulated CFT and mean dot distance for extrusion speed of 1 and 4kb/s.

A) The average search time between two monomers separated by 360 monomers (corresponding to a genomic distance of 360 kb) in simulated polymers with loop extrusion at v=1kb/s, shown for different values of loop size (λ) and loop separation (d). Dashed lines indicate the experimentally measured search times in cells with condensin (-Auxin, green) and without condensin (+Auxin, grey), with shaded regions representing the corresponding error bars. **B)** Same as (A), but showing the average spatial distance between the two monomers instead of search time. **C)** The same simulation data points as in A) and B), but with dot distance plotted against search time. Simulations where both the dot distance and search time fall within 1.5 times the experimental error are annotated. **D-F** Same than A-C for v = 4kb/s.

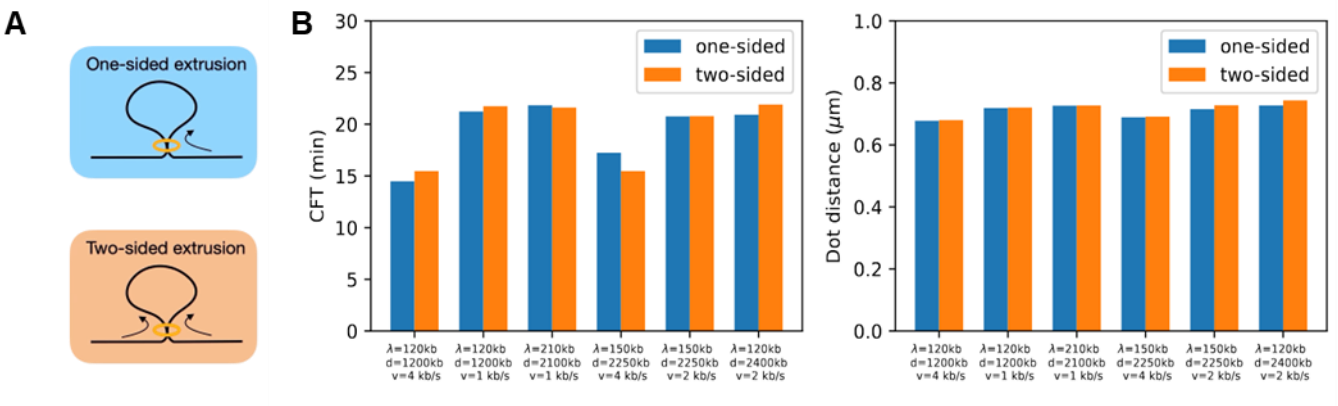

Supplementary Fig. 9. Comparison of one-sided and two-sided extrusion. A) Cartoon of the two models. **B)** Barplots show the mean contact formation time (left) and mean dot distance (right) across representative parameter sets. Results demonstrate that one-sided (blue) and two-sided (orange) extrusion yield indistinguishable average distance and search time for all tested processivity, separation, and velocity values.

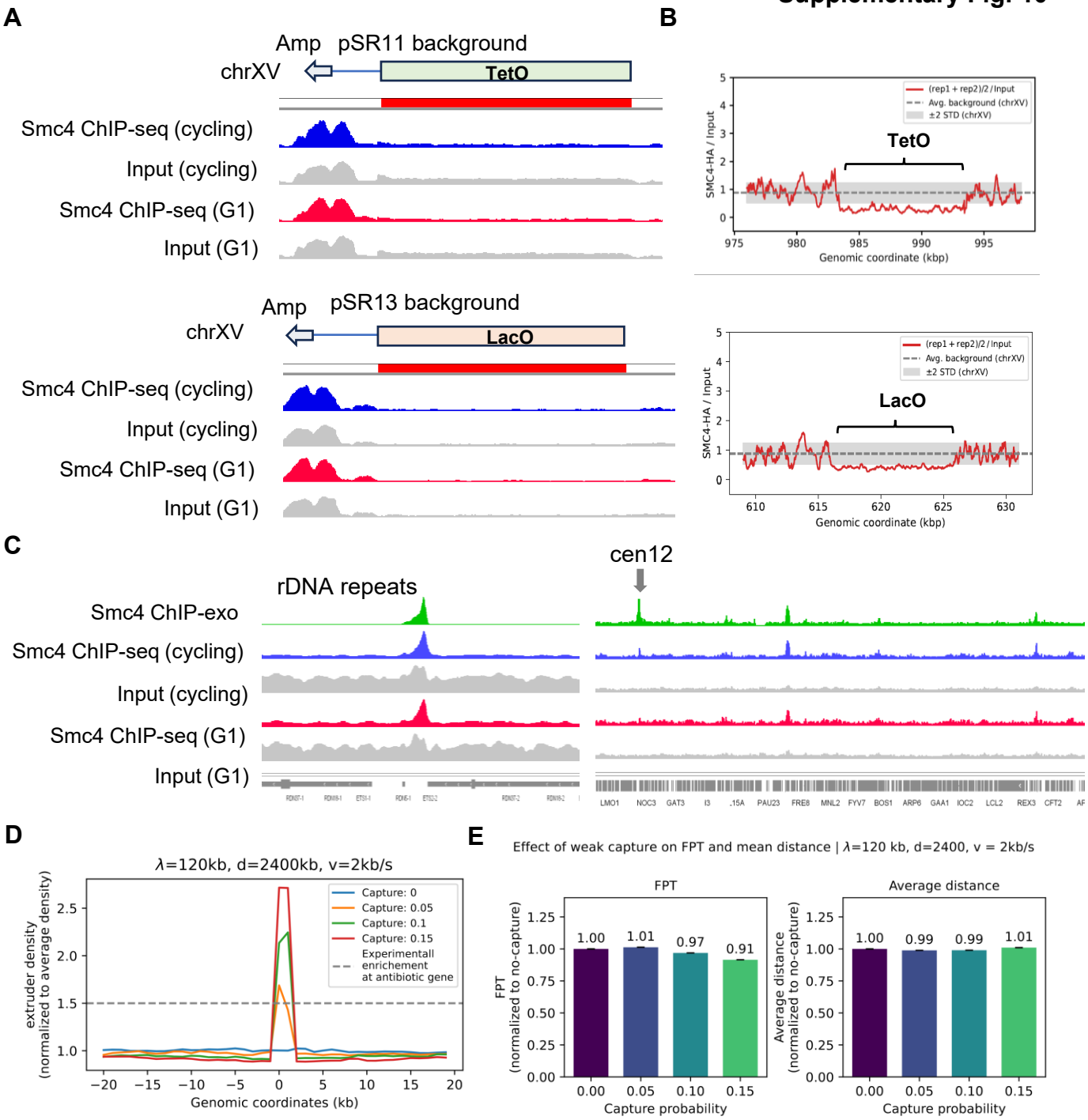

Supplementary Fig. 10. TetO/LacO arrays do not form strong barriers for condensin loop extrusion in our system. **A&B)** Smc4 ChIP-seq signal at the two arrays. Due to their repetitive nature, reads for both the ChIP and input sample are randomly distributed over the arrays. Normalized ChIP signals (ChIP/input) are shown in B. Smc4 density within both arrays is lower than the genome-wide average, while the flanking regions exhibit very weak Smc4 accumulation, especially over the Amp gene. **C)** Smc4 ChIP-seq profiles over the rDNA locus (left) and near the chrXII centromere (right). The observed enrichment is consistent with previous ChIP-exo data (Rossi et al., 2021), validating the ChIP-seq measurements. **D)** Simulated condensin ChIP-seq profiles at the Amp gene for weak capture probabilities. Condensin is transiently trapped at array boundaries with a mean dwell time of 60 s. Capture probabilities of 5–15% generate condensin enrichment comparable to or exceeding experimentally measured levels at the Amp gene, indicating that the simulated barriers operate within a realistic or stronger-than-observed regime. Simulations were performed with processivity = 120 kb, separation d = 2400 kb, and extrusion speed v = 2 kb/s. **E)** First-passage time (FPT, left) and average array distance (right) as a function of capture probability, normalized to the no-capture case. Using the same parameters as in (D), weak capture has negligible effects on mean distance and only minimal effects on FPT.

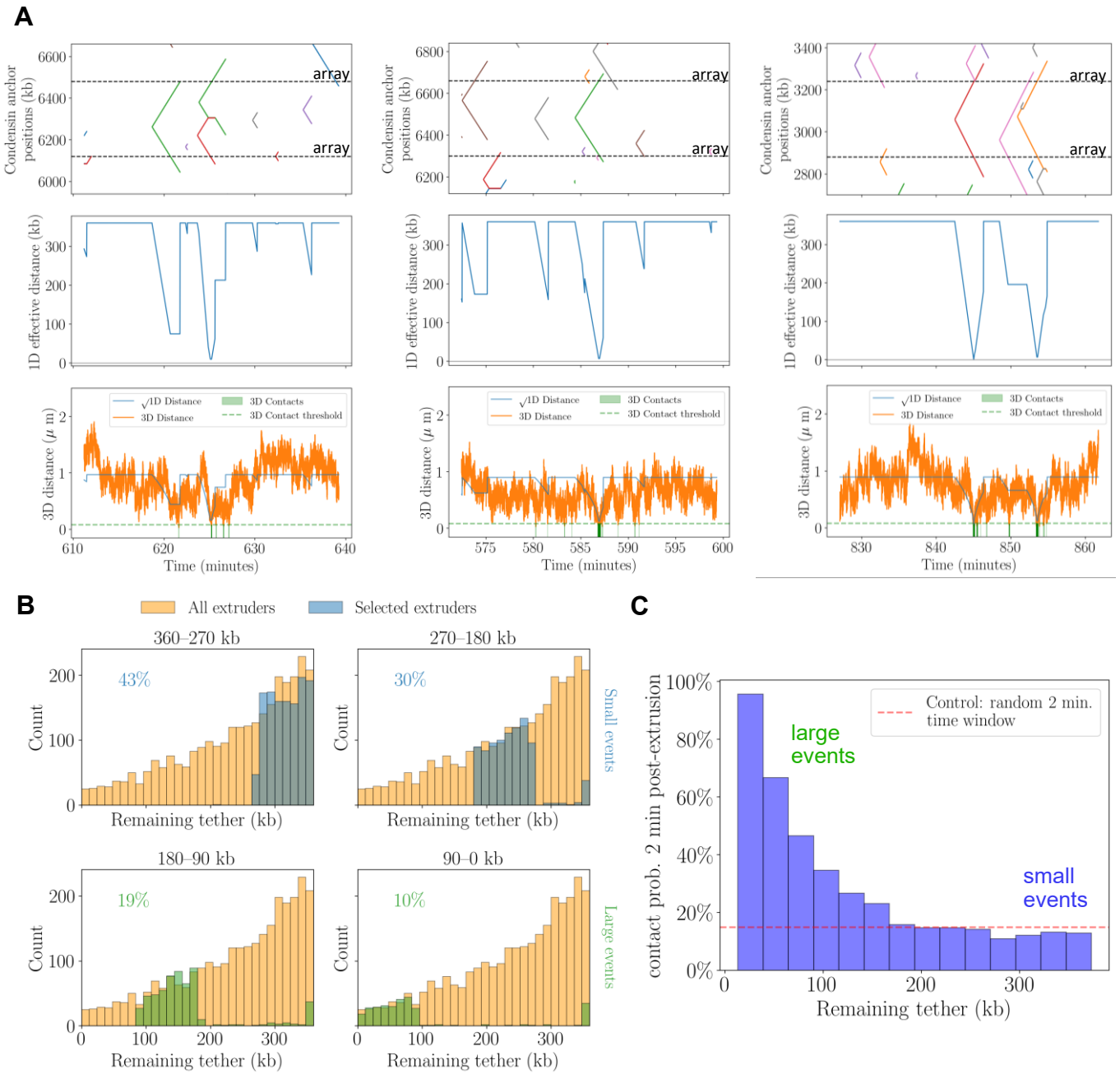

Supplementary Fig. 11. Contribution to CICI formation by large vs small extrusion events. A) Each panel shows representative simulated extrusion events where condensin reduces the effective 1D genomic distance between the arrays, triggering potential 3D contact. *Top*: positions anchored by condensin over time, with dashed lines marking the genomic positions of the arrays. *Middle*: 1D effective distance between the arrays. *Bottom*: corresponding 3D distance (orange), plotted alongside the re-scaled square root of the 1D distance (blue). Green shaded areas indicate periods where the 3D distance drops below the contact threshold. **B)** Histograms of minimal remaining tether during extrusion events. All extrusion events (orange) are shown alongside those retained for simulation under size-selective extruder removal (blue: small events; green: large events). Each panel corresponds to a different range polymer simulations isolating the effect of extrusion events of specific sizes (see Methods and Fig. 7A). **C)** Contact probability (in percents) within a 2-min window following the point of minimal 1D distance during extrusion events, binned by the minimal tether length remaining between the two loop anchors (x-axis). Blue bars represent the probability that the two loci come into 3D contact within a 2 minute time window after extrusion. Dashed red line indicates the baseline probability of contact at random times, computed by averaging contact formation over 2 minute random time windows.

Supplementary Table 1

Plasmid	Note	Note
pSR11	192X TetO with a TRP1 marker	Rohner et al.
pSR13	256X LacO with a LEU2 marker	
pSR11-S1	pSR11 plasmid with homologous sequence from Chr15::433546	This study
pSR11-S2	pSR11 plasmid with homologous sequence from Chr15::612715	
pSR11-S3	pSR11 plasmid with homologous sequence from Chr15::793958	
pSR11-S4	pSR11 plasmid with homologous sequence from Chr15::966177	
pSR11-S5	pSR11 plasmid with homologous sequence from Chr4::916282	
pSR11-S6	pSR11 plasmid with homologous sequence from Chr4::1166682	
pSR11-S7	pSR11 plasmid with homologous sequence from Chr4::150277	
pSR11-S8	pSR11 plasmid with homologous sequence from Chr4::168727	
pSR11-S9	pSR11 plasmid with homologous sequence from Chr4::306772	
pSR13-S1	pSR13 plasmid with homologous sequence from Chr15::433546	
pSR13-S4	pSR13 plasmid with homologous sequence from Chr15::966175	
pSR13-S5	pSR13 plasmid with homologous sequence from Chr4::916282	
pSR13-S6	pSR13 plasmid with homologous sequence from Chr4::1389000	
pSR13-S7	pSR13 plasmid with homologous sequence from Chr4::624000	
pSR13-S8	pSR13 plasmid with homologous sequence from Chr4::497047	
pSR13-S9	pSR13 plasmid with homologous sequence from Chr4::616331	
posTIR1_ura	For expressing osTIR1	
pscAID_rc_hpxMX_smc4	For tagging Smc4 with auxin-degron	
pscAID_rc_hpxMX_brn1	For tagging Brn1 with auxin-degron	
Strain	**Genotype**	**Note**
yMD215	MAT<u>a</u>, tor1-1, fpr::NAT, bar1, HIS3::REV1pr-tetR-mCherry-REV1pr-LacI-GFP, ADE2::REV1pr-LacI-FKBP12-REV1pr-TetR-FRB	Background, Du et al.
yFZ103	MAT<u>a</u>, tor1-1, fpr::NAT, bar1, HIS3::REV1pr-tetR-mCherry-REV1pr-LacI-GFP, ADE2::REV1pr-LacI-FKBP12-REV1pr-TetR-FRB, Chr15::433546_LacO, Chr15::966177_TetO	Pair 1
yFZ101	MAT<u>a</u>, tor1-1, fpr::NAT, bar1, HIS3::REV1pr-tetR-mCherry-REV1pr-LacI-GFP, ADE2::REV1pr-LacI-FKBP12-REV1pr-TetR-FRB, Chr15::433546_LacO, Chr15::612715_TetO	Pair 2
yFZ102	MAT<u>a</u>, tor1-1, fpr::NAT, bar1, HIS3::REV1pr-tetR-mCherry-REV1pr-LacI-GFP, ADE2::REV1pr-LacI-FKBP12-REV1pr-TetR-FRB, Chr15::433546_LacO, Chr15::793958_TetO	Pair 3
yFZ107	MAT<u>a</u>, tor1-1, fpr::NAT, bar1, HIS3::REV1pr-tetR-mCherry-REV1pr-LacI-GFP, ADE2::REV1pr-LacI-FKBP12-REV1pr-TetR-FRB, Chr15::966175_LacO, Chr15::612715_TetO	Pair 4, Hi-C WT
yFZ113YL	MAT<u>a</u>, tor1-1, fpr::NAT, bar1, HIS3::REV1pr-tetR-mCherry-REV1pr-LacI-GFP, ADE2::REV1pr-LacI-FKBP12-REV1pr-TetR-FRB, Chr4::1389000_LacO, Chr4::916282_TetO	Pair 5
yFZ114YL	MAT<u>a</u>, tor1-1, fpr::NAT, bar1, HIS3::REV1pr-tetR-mCherry-REV1pr-LacI-GFP, ADE2::REV1pr-LacI-FKBP12-REV1pr-TetR-FRB, Chr4::624000_LacO, Chr4::1166682_TetO	Pair 6
yMD266	MAT<u>a</u>, tor1-1, fpr::NAT, bar1, HIS3::REV1pr-tetR-mCherry-REV1pr-LacI-GFP, ADE2::REV1pr-LacI-FKBP12-REV1pr-TetR-FRB, Chr4::497047_LacO, Chr4::150277_TetO	Pair 7
yYL81	MAT<u>a</u>, tor1-1, fpr::NAT, bar1, HIS3::REV1pr-tetR-mCherry-REV1pr-LacI-GFP, ADE2::REV1pr-LacI-FKBP12-REV1pr-TetR-FRB, Chr15::966175_LacO, Chr15::168727_TetO	Pair 8
yFZ104	MAT<u>a</u>, tor1-1, fpr::NAT, bar1, HIS3::REV1pr-tetR-mCherry-REV1pr-LacI-GFP, ADE2::REV1pr-LacI-FKBP12-REV1pr-TetR-FRB, Chr15::433546_LacO, Chr4::916282_TetO	Pair 9
yFZ105	MAT<u>a</u>, tor1-1, fpr::NAT, bar1, HIS3::REV1pr-tetR-mCherry-REV1pr-LacI-GFP, ADE2::REV1pr-LacI-FKBP12-REV1pr-TetR-FRB, Chr15::433546_LacO, Chr4::1166682_TetO	Pair 10
yFZ109	MAT<u>a</u>, tor1-1, fpr::NAT, bar1, HIS3::REV1pr-tetR-mCherry-REV1pr-LacI-GFP, ADE2::REV1pr-LacI-FKBP12-REV1pr-TetR-FRB, Chr15::966175_LacO, Chr4::916282_TetO	Pair 11
yFZ110	MAT<u>a</u>, tor1-1, fpr::NAT, bar1, HIS3::REV1pr-tetR-mCherry-REV1pr-LacI-GFP, ADE2::REV1pr-LacI-FKBP12-REV1pr-TetR-FRB, Chr15::966175_LacO, Chr4::1166682_TetO	Pair 12
yMD282	MAT<u>a</u>, tor1-1, fpr::NAT, bar1, HIS3::REV1pr-tetR-mCherry-REV1pr-LacI-GFP, ADE2::REV1pr-LacI-FKBP12-REV1pr-TetR-FRB, Chr12::616331_LacO, Chr12::306772_TetO	Pair 13
yFZ103-smc4	MAT<u>a</u>, tor1-1, fpr::NAT, bar1, HIS3::REV1pr-tetR-mCherry-REV1pr-LacI-GFP, ADE2::REV1pr-LacI-FKBP12-REV1pr-TetR-FRB, Chr15::433546_LacO, Chr15::966177_TetO, HO::OsTIR1-URA3, SMC4-V5-AID-Hyg	Pair 1, Smc4 depletion
yFZ107-smc4	MAT<u>a</u>, tor1-1, fpr::NAT, bar1, HIS3::REV1pr-tetR-mCherry-REV1pr-LacI-GFP, ADE2::REV1pr-LacI-FKBP12-REV1pr-TetR-FRB, Chr15::966175_LacO, Chr15::612715_TetO, HO::OsTIR1-URA3, SMC4-V5-AID-Hyg	Pair 4, Smc4 depletion, Hi-C
yFZ113YL-smc4	MAT<u>a</u>, tor1-1, fpr::NAT, bar1, HIS3::REV1pr-tetR-mCherry-REV1pr-LacI-GFP, ADE2::REV1pr-LacI-FKBP12-REV1pr-TetR-FRB, Chr4::1389000_LacO, Chr4::916282_TetO, HO::OsTIR1-URA3, SMC4-V5-AID-Hyg	Pair 5, Smc4 depletion
yMD266-smc4	MAT<u>a</u>, tor1-1, fpr::NAT, bar1, HIS3::REV1pr-tetR-mCherry-REV1pr-LacI-GFP, ADE2::REV1pr-LacI-FKBP12-REV1pr-TetR-FRB, Chr4::497047_LacO, Chr4::150277_TetO, HO::OsTIR1-URA3, SMC4-V5-AID-Hyg	Pair 7, Smc4 depletion
yYL81-smc4	MAT<u>a</u>, tor1-1, fpr::NAT, bar1, HIS3::REV1pr-tetR-mCherry-REV1pr-LacI-GFP, ADE2::REV1pr-LacI-FKBP12-REV1pr-TetR-FRB, Chr15::966175_LacO, Chr15::168727_TetO, HO::OsTIR1-URA3, SMC4-V5-AID-Hyg	Pair 8, Smc4 depletion
yFZ104-smc4	MAT<u>a</u>, tor1-1, fpr::NAT, bar1, HIS3::REV1pr-tetR-mCherry-REV1pr-LacI-GFP, ADE2::REV1pr-LacI-FKBP12-REV1pr-TetR-FRB, Chr15::433546_LacO, Chr4::916282_TetO, HO::OsTIR1-URA3, SMC4-V5-AID-Hyg	Pair 9, Smc4 depletion
yFZ105-smc4	MAT<u>a</u>, tor1-1, fpr::NAT, bar1, HIS3::REV1pr-tetR-mCherry-REV1pr-LacI-GFP, ADE2::REV1pr-LacI-FKBP12-REV1pr-TetR-FRB, Chr15::433546_LacO, Chr4::1166682_TetO, HO::OsTIR1-URA3, SMC4-V5-AID-Hyg	Pair 10, Smc4 depletion
yFZ110-smc4	MAT<u>a</u>, tor1-1, fpr::NAT, bar1, HIS3::REV1pr-tetR-mCherry-REV1pr-LacI-GFP, ADE2::REV1pr-LacI-FKBP12-REV1pr-TetR-FRB, Chr15::966175_LacO, Chr4::1166682_TetO,HO::OsTIR1-URA3, SMC4-V5-AID-Hyg	Pair 12, Smc4 depletion
yMD282-brn1	MAT<u>a</u>, tor1-1, fpr::NAT, bar1, HIS3::REV1pr-tetR-mCherry-REV1pr-LacI-GFP, ADE2::REV1pr-LacI-FKBP12-REV1pr-TetR-FRB, Chr12::616331_LacO, Chr12::306772_TetO, HO::OsTIR1-URA3, Brn1-V5-AID-Hyg	Pair 13, Brn1 depletion